

This document is downloaded from DR-NTU, Nanyang Technological University Library, Singapore.

Title	Design and Development of Cryo-Adsorption Chamber for the Measurement of Methane Uptakes on Activated Carbons and MOFs
Author(s)	Chakraborty, Anutosh; Sun, Baichuan; Ali, Syed Muztuza; Fan, Wu
Citation	Chakraborty, A., Sun, B., Ali, S. M., & Fan, W. (2014). Design and Development of Cryo-Adsorption Chamber for the Measurement of Methane Uptakes on Activated Carbons and MOFs. Proceedings of the 7th Asian Conference on Refrigeration and Air Conditioning.
Date	2014
URL	<a href="http://hdl.handle.net/10220/42265">http://hdl.handle.net/10220/42265</a>
Rights	© 2014 The Author(s) (Proceedings of the 7th Asian Conference on Refrigeration and Air Conditioning). This paper was published in Proceedings of the 7th Asian Conference on Refrigeration and Air Conditioning and is made available as an electronic reprint (preprint) with permission of The Author(s) (Proceedings of the 7th Asian Conference on Refrigeration and Air Conditioning). The published version is available at: [ <a href="https://www.scribd.com/document/228933342/Design-and-Development-of-Crioadsorption-chamber-for-methane-storage-on-MOF">https://www.scribd.com/document/228933342/Design-and-Development-of-Crioadsorption-chamber-for-methane-storage-on-MOF</a> ]. One print or electronic copy may be made for personal use only. Systematic or multiple reproduction, distribution to multiple locations via electronic or other means, duplication of any material in this paper for a fee or for commercial purposes, or modification of the content of the paper is prohibited and is subject to penalties under law.

## DESIGN AND DEVELOPMENT OF CRYO-ADSORPTION CHAMBER FOR THE MEASUREMENT OF METHANE UPTAKES ON ACTIVATED CARBONS AND MOFS

Anutosh Chakraborty\*, Baichuan Sun, Syed Muztuza Ali, and Wu Fan

*School of Mechanical and Aerospace Engineering, Nanyang Technological University, 50 Nanyang Avenue, Singapore 639798, Republic of Singapore*

**ABSTRACT:** We have designed and developed the cryo-adsorption chamber to measure methane uptakes on various MOFs and activated carbons for the temperatures ranging from 120 K to 300 K and pressures up to 10 bar with temperature and pressure controls. The experimentally measured data are fitted with the modified Langmuir adsorption (MLA) equation. The MLA isotherm describes all of the isotherm experimental data within the acceptable error ranges. The thermo-physical properties of activated carbon (type Maxsorb III) and MOFs (Fe-BTC) are also presented in this paper. The present isotherm data are compared with other published data and showed the superiority of the present findings in terms of uptake capacity employing the newly designed metal organic frameworks (MOFs).

### 1. INTRODUCTION

Over the last decade, metal-organic frameworks (MOFs) and activated carbons have emerged as an important class of new materials for gas storage or gas separation tasks as well as catalysis and industrial applications [1]. This paper presents the experimental methods for methane adsorption onto pitch-based activated carbon type Maxsorb III and metal organic frameworks (MOFs) for understanding methane capture and storage at temperatures ranging from 120 to 160 K and pressures up to 10 bar. Temperatures at cryogenic ranges are maintained using a purpose-built cryostat. The volumetric technique is employed to measure the adsorption uptake data. These data are important in the study of adsorbed natural gas (ANG) storage system when low temperature natural gas is charged into the adsorptive gas storage. In the ANG storage system, the adsorbate molecules are captured in the pores of the adsorbent with an evolution of heat since adsorbate (gas) molecules are denser on the adsorbent surface than in the bulk phase. Consequently, the gas storage vessel requires a cooling system during gas charge to remove the heat of adsorption so as to increase the storage capacity. If the methane is in liquid form or at very low temperature, a dedicated cooling system is not required. Since transcontinental transport of natural gas is only as LNG, an ANG system with LNG cooled charging will be an ideal proposition. This tech and it helps to avoid the complexity of (i) re-gasification of the LNG to ambient condition, (ii) using compressor to charge the gas in the ANG vessel, and (iii) the cooling arrangement. To implement this, the adsorption characteristics of methane + various porous adsorbents like MOFs must be known

at low temperature ranges. However, the adsorption parameters of methane for sub and super-critical temperatures ( $>190.56$  K) on activated carbons are available in the literature [2-5]. The adsorption parameters are evaluated from the measured uptake data using the modified Langmuir isotherm model. The heat of adsorption, which is concentration and temperature dependent, are also extracted from the isotherm data.

### 2. CRYOGENIC EXPERIMENTAL INVESTIGATION

The experimental apparatus is described in two sections: (i) the volumetric apparatus to measure the adsorption uptake for an adsorbate+ adsorbent pair at various isothermal conditions and (ii) the cryostat to maintain the adsorption cell at constant temperature in cryogenic states.

#### 2.1 Volumetric Apparatus

The experimental apparatus consists of a stainless steel adsorption cylinder and a charging cylinder with internal volume of  $183.842 \pm 0.159$  ml and  $323.347 \pm 0.273$  ml. The schematic for the adsorption and charging chambers where the adsorption occurs are shown in Figure 1. Two pressure transducers (Kyowa-PGS-200KA) are mounted on the stainless steel adsorption and charging chambers by  $6.35 \pm 10^{-3}$  m stainless steel tube. The uncertainty of the pressure transducers are of 0.2 % in measurement. The temperature of the adsorption and charging chambers are recorded using class-A Pt 100 RTDs with estimated uncertainty of  $\pm 0.15$  °C. The RTD in the adsorption cell is in contact with the adsorbent materials to enable direct temperature measurement, by wrapping the adsorbents with metal

mesh onto the RTD probes. All temperature and pressure data are logged into the Agilent 34972A LXI data acquisition every 1 s to enable real time monitoring of the adsorption uptake. A set of compression fittings to withstand pressure of larger than 40 MPa are used.

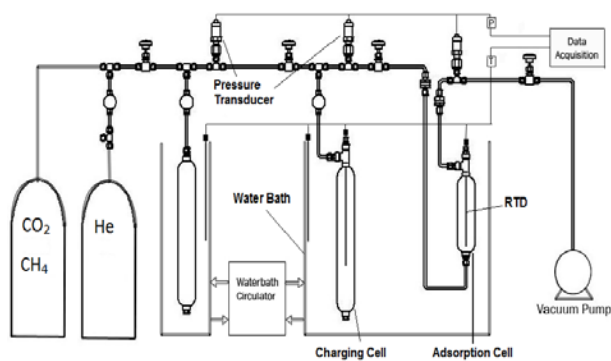


Fig. 1. Schematic diagram of a typical volumetric apparatus for isotherm

The adsorption and charging chambers are immersed in a bulk of circulated water at a controlled constant temperature until it is thermally stabilized before the experiments are conducted. The heating/refrigeration circulator is used, and its accuracy to maintain the preset temperature is  $\pm 0.01$  °C. With this design and mechanism, we assume that the experiment is performed isothermally with no significant temperature fluctuation. Helium gas with purity of 99.999 %, supplied in small cylinder, is used to remove residual gases on the surfaces of adsorption chamber before the experiment. CH<sub>4</sub> gases with purity of 99.999 %, also provided in small cylinder, are used in the experiment.

## 2.2 Cryostat Setup

In order to conduct adsorption isotherm experiments at cryogenic temperature ranges of 110 - 220 K, a cryogenic adsorption setup was designed, developed and fabricated, and this is shown in Figure 2. The setup consists of an adsorption reactor chamber, made up with oxygen-free high thermal conductivity (OFHC) copper for optimum isothermal operation by its high thermal conductivity. The internal volume of the chamber is 100 ml and the indium wire seal is used to prevent leakage of adsorbate gas. Liquid nitrogen is introduced from the 50 liter aluminum dewar by cryogen entry and flow through the convey hose, which is isolated from the ambient by evacuated sleeve outside. Following that liquid nitrogen flows out from the cryogen venting port, and heat is drawn out from the react chamber by the copper stick led to the liquid nitrogen flow cycle. The copper stick is isolated from the ambient by vacuum shroud. Temperatures inside the chamber are expected to be cooled down to 77 K in this way. Two cartridge heaters are mounted into the lower wall of the reactor at 180 degrees from each other to increase the temperature of the reactor from 77 K to 420 K depending on experimental requirements. The heaters are manipulated by Model 22C cryogenic temperature controller with enhanced PID adjustor. An internal spring and pressure plate are applied to hold adsorbent materials and push them up against the DT-670B-CU-HT silicon diode

thermometers, so that the temperature of the adsorbent could be measured directly. The working pressure range of this setup is 0 - 15 bar, which is controlled by the gas source regulator. The pressure changes are recorded by GS4200-USB digital pressure transducer with an error of  $\pm 0.1\%$ . The cryogenic adsorption isotherms of hydrogen and methane are to be studied with this setup.

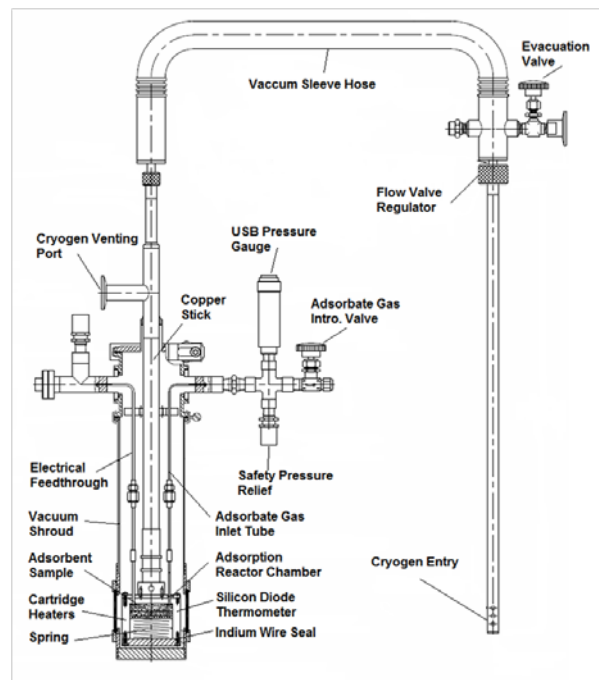


Fig. 2 Schematic diagram of cryogenic adsorption set-up

## 2.3 Adsorbate Uptake Measurements

The data collected from the volumetric adsorption experiment are pressure and temperature readings of the charging and the adsorption cells shown in Figures 1 and 2. These readings need to be reduced into uptake data and be fitted into isotherm and kinetics equations. In order to calculate the uptake, additional information such as the volume of the charging and the adsorption cells, and the density of the gas as a function of temperature and pressure, are required. To get the volume of the charging and the adsorption cells, both liquid volume calibration and gas volume calibration were conducted. In liquid calibration method, two sub-methods were applied, 1) volume of water filled into the cells measurement, or 2) liquid within the cells gravimetric measurement. In this research, both methods were performed to evaluate the suitability and accuracy of each chamber. The liquid calibration is conducted on the charging cell, and the adsorption cell is calibrated by gas calibration. Therefore, the charging cell has to be calibrated very precisely, as it will affect the measurements of the subsequent gas calibration. As the adsorbents are later put inside of the adsorption cell, the volume taken by the adsorbent samples  $V_{solid}$  are needed to be deducted. Firstly, liquid water was injected into the charging cell with a syringe, and amounts of injected by syringe and drained from the measuring cylinder are recorded. Secondly, dry cells under vacuum were weighed and then water was charged into the cell, and weighed again together. The difference on weight is seen

as water that occupies all space inside the cell. Finally, after volume of charging cell  $V_{char}$  has been determined by liquid calibration, high purity methane gas was filled into the charging cell and the equilibrium temperature and pressure were recorded. By allowing  $CH_4$  to travel to adsorption cell, the value of T and P were recorded again. With the density of  $CH_4$  as function of temperature and pressure based on real gas model, the volume of adsorption cell  $V_{react}$  was determined by the difference between the total volume of charging and adsorption cells  $V_{char} + V_{react}$  and  $V_{char}$ . All calibration steps were repeated for 5 times to maintain the precision and accuracy.

The density of gas, with respect to temperature and pressure,  $\rho(T_{read}, P_{read})$ , is obtained from NIST Standard Reference Database 23 of Version 8.0 at specified state points. The adsorbed mass is determined by the volumetric method experiment. At the first step, there is remaining gas inside the adsorption cell:

$$x_{remain} = \rho_{react}(T_{read}, P_{read}) \cdot V_{react}$$

Following adsorbate gas is dosed into the charging cell:

$$x_{char} = \rho_{char}(T_{read}, P_{read}) \cdot V_{char}$$

After the adsorption reaction, the residual mass is left in the apparatus as:

$$x_{res} = \rho_{res}(T_{read}, P_{read}) \cdot (V_{char} + V_{react})$$

Therefore, the subsequent adsorbed mass is calculated with the following equation

$$x_a = x_{remain} + x_{char} - x_{res}$$

The amount of adsorbed mass at equilibrium after each charging pressure will be accumulated to obtain the uptake of adsorption under each equilibrium pressure. These cumulative adsorbed uptakes are plotted with the absolute equilibrium pressure or the relative pressure to saturated value, to get experimental adsorption isotherm chart.

### 3. ADSORBATE AND ADSORBENT MATERIALS

#### 3.1 $CH_4$ Adsorbate

The ultra pure methane sample supplied by SOXAL (Singapore Oxygen Air Liquid Pte Ltd) was used for the present experiment. The purity grade of the sample used was 99.9995% of  $CH_4$  with the supplier stated impurity levels as follows:  $N_2 < 4$  ppm,  $O_2 < 0.5$  ppm, OHC  $< 0.5$  ppm,  $C_2H_6 < 0.5$  ppm, and  $H_2O < 1$  ppm.

#### 3.2 MOFs and Activated Carbons

MOF materials are synthesized in a self-assembly process in which metal vertices are connected by organic linkers. The wide variety of possible linker and corner units results in a large number of metal-organic frameworks. Over 13000 crystalline, extended metal containing frameworks are catalogued in the Cambridge Structure Database [6]. The chemical composition, building blocks and pore structure of typical MOFs are shown in Figure 3. More and more porous metal-organic materials are emerging that show promising properties. The modular building process allows systematic tailoring

of the physical and chemical properties of the cavities, chemical composition, building blocks and pore structure of the MOFs.

The texture of the MOFs composite and activated carbon (type maxsorb-III) can be observed by scanning electron microscopy (SEM) images as presented in Fig. 4. Fig. 4(a) shows a SEM photograph of Maxsorb III, where the surface structure is observed to be flake-like layers with porous volumes entrenched between the layers. On the other hand, The MOF (type HKUST-1) is clearly visible with a crystalline phase and it shows that crystals of HKUST-1 have smooth surfaces and have an average size of 10 nm as shown in Fig. 4(b).

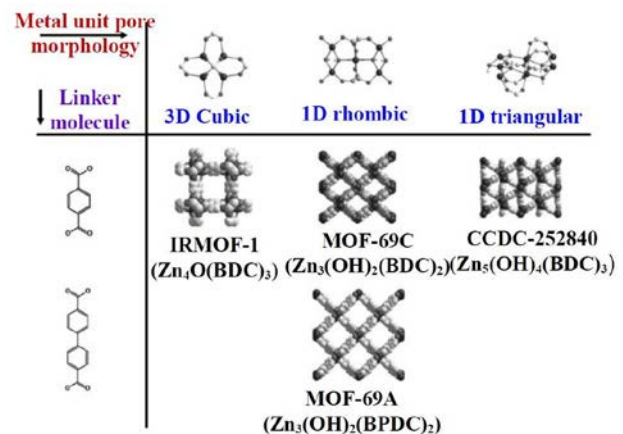


Fig. 3. Chemical composition, building blocks and pore structure of the MOFs

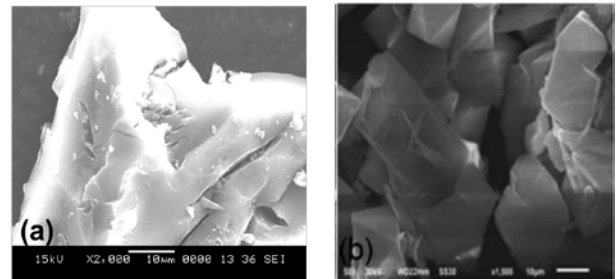


Fig. 4 SEM pictures of (a) Maxsorb-III and (b) HKUST-1

Table 1 Thermo-Physical Properties

Properties	Maxsorb III	IRMOF-1
BET surface area ( $m^2/kg$ )	$3.14 \times 10^6$	$2.099 \times 10^6$
total pore volume ( $m^3/kg$ )	$2.01 \times 10^{-4}$	$1.69 \times 10^{-4}$
micro pore volume ( $m^3/kg$ )	$1.79 \times 10^{-4}$	$1.37 \times 10^{-4}$
average pore diameter ( $\text{\AA}$ )	20.08	10.9/14.3

Table 1 tabulates the properties of Maxsorb III and MOFs, such as the Brunauer-Emmett-Teller (BET) surface area, pore size, pore volume, porosity, and the skeletal density. These thermo-physical properties were

measured using an Autosorb machine: The surface area was calculated by the BET method from the N<sub>2</sub> adsorption isotherm data, which has been performed at 77.3 K. The pore size distribution (PSD) has been obtained by the nonlocal density functional theory (NLDFT) method.

#### 4. MODIFIED LANGMUIR EQUATION

From the perspective of adsorption energy distribution, the Langmuir adsorption isotherm equation is modified and reformulated on the basis of Fermi-Dirac distribution function. The proposed isotherm model including the loading effect ( $\beta$ ), the adsorbent-adsorbate interaction ( $n$ ) and the surface structural heterogeneity factors ( $m$ ), overcomes the limitations of the existing isotherm models such as Langmuir, Tóth or Dubinin equations. The modified equation is written as [7]

$$\theta = \frac{\beta \left( \frac{P}{\varphi^*} \right)}{\left[ 1 + \left( \beta^m - \alpha \right) \left( \frac{P}{\varphi^*} \right)^m \right]^{\frac{1}{m}}}, \quad (1)$$

where  $\theta (= q/q^o)$  defines the surface coverage,  $P$  is the pressure,  $T$  indicates the temperature,  $q$  is the amount of adsorbate uptake and  $q^o$  stands for the limiting uptake.  $\varphi^*$  is the factor that depends on the isosteric heat of adsorption and temperature. Here

$$\frac{P}{\varphi^*} = \left( \frac{P}{P_s} \right) \exp \left\{ \frac{\phi_m}{RT} \left[ 1 - \left( \frac{P}{P_s} \right)^n \right] + z \right\},$$

and the exponential term of compressibility factor ( $z$ ) is given by  $\alpha = \{1/\exp(z)\}^m$ .

#### 5. RESULTS AND DISCUSSION

The experimentally measured uptake data at different isothermal conditions (constant  $T$ ) for the adsorption of methane on Maxsorb III are shown in Figure 5. The isotherm data have been measured for temperatures ranging from (120 to 150) K and pressures up to 1.0 MPa and regressed using the modified Langmuir model with an average regression error of 6%. The solid lines in Figure 5 represent the isotherms calculated from the MLA model using the regressed adsorption parameters ( $q^o = 0.56$  kg/kg,  $\alpha = 0.135$ ,  $m = 2$ ,  $n = 0.15$ ,  $\beta = 1$  and  $\phi_m = 250$  kJ/kg). As the Maxsorb III adsorbent is highly microporous and heterogeneous in the surface structure, the MLA isotherm model provides a good representation due to the accountability of the heterogeneity parameter ( $m$ ).

Methane sorption isotherms on Fe<sub>3</sub>(BTC)<sub>2</sub> have been measured at temperatures between 130 and 140 K and pressures up to 10 bar and are provided in Fig. 6. They show a generally decreasing trend with temperature from 0.1 to 0.8 kg CH<sub>4</sub>/kg MOF at 140 K. After passing a maximum value, the excess sorption isotherms in Fig. 6 decrease slightly until the final pressure value is reached. This declination nature can be attributed to a volumetric effect (non-negligible volume

of the adsorbed phase) that needs to be considered when calculating absolute sorption capacities. The experimental data are fitted with the modified Langmuir equation as shown in equation (1).

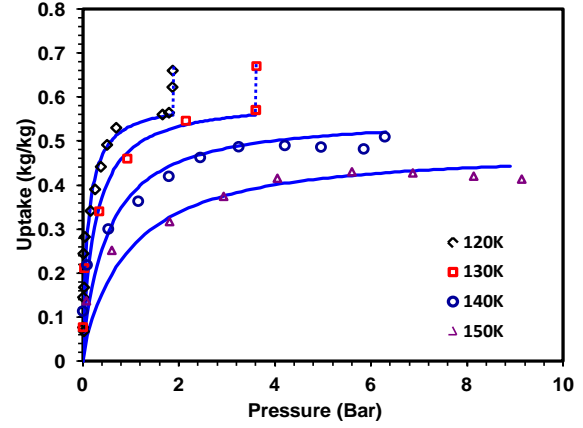


Fig. 5 CH<sub>4</sub> uptakes on activated carbons (type Maxsorb-III) for the temperatures ranging from 120 K to 150 K and pressures up to 10 bar.

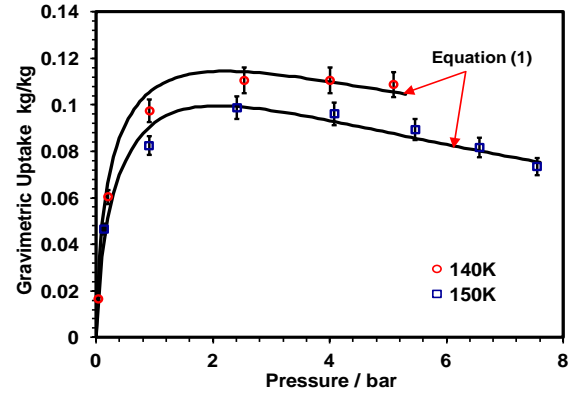


Fig. 6. CH<sub>4</sub> uptakes on Fe based MOFs for the temperatures of 140 and 150 K and pressures up to 8 bar.

#### 6. CONCLUSIONS

The conventional volumetric apparatus has been successfully incorporated with a specially designed cryostat where the uptake of pure methane on Maxsorb III and MOFs has been measured for cryogenic temperatures ranging from (120 to 150) K and pressure up to 10 bar. The experimental results have been regressed with the modified Langmuir isotherm model and found to be well described with regression error of 5%. The uptake results provide the necessary information about the changing pressure and temperature for ANG storage systems, especially when the natural gas is charged from the LNG terminal at near cryogenic temperatures.

#### REFERENCES

- [1] T. Düren, How does the pore morphology influence the adsorption performance of metal-organic frameworks? A molecular simulation study of methane and ethane adsorption in Zn-MOFs, Studies in Surface Science and Catalysis, Vol. 170, pp. 2042–2047, 2007.
- [2] K. A. Rahman, W.S. Loh, H. Yanagi, A. Chakraborty, B. B. Saha, W. G. Chun, and K. C. Ng, Experimental

Adsorption Isotherm of Methane onto Activated Carbon at Sub and Supercritical Temperatures, *J. Chem. Eng. Data*, Vol. 55, pp. 4961–4967, 2010.

[3] S.K. Bhatia, A. L. Myers, Optimum Conditions for Adsorptive Storage, *Langmuir*, Vol. 22, pp.1688–1700, 2006.

[4] X. D. Yang, Q. R. Zheng, A. Z. Gu, X. S. Lu, Experimental studies of the performance of adsorbed natural gas storage system during discharge. *Applied Thermal Engineering*, Vol. 25, pp. 591–601, 2005.

[5] K. R. Matranga, A. L. Myers, E. D. Glandt, Storage of natural gas by adsorption on activated carbon. *Chemical Engineering Science*, Vol. 47, pp. 1569–1579, 1992.

[6] L. Li, X. L. Liu, H. Y. Geng, B. Hu, G. W. Song, and Z. S. Xu, A MOF/graphite oxide hybrid (MOF: HKUST-1) material for the adsorption of methylene blue from aqueous solution, *Journal of Materials Chemistry A*, Vol. 1, pp. 10292–10299, 2013.

[7] B. Sun, A. Chakraborty, On Thermodynamics of a Novel Adsorption Isotherm Equation, *Innovative Materials for Processes in Energy Systems 2013*, Fukuoka, Japan, p. 344 – 350, 2013